Latest Advances of Model Predictive Control in Electrical Drives. Part II: Applications and Benchmarking with Classical Control Methods

Jose Rodriguez, *Life Fellow, IEEE,* Cristian Garcia, *Member, IEEE,* Andres Mora, *Member, IEEE,* S. Alireza Davari, *Senior Member, IEEE,* Jorge Rodas, *Senior Member, IEEE,* Diego F. Valencia, *Member, IEEE,* Mahmoud Elmorshedy, *Member, IEEE,* Fengxiang Wang, *Senior Member, IEEE,* Kunkun Zuo, Luca Tarisciotti, *Member, IEEE,* Freddy Flores-Bahamonde, *Member, IEEE,* Wei Xu, *Senior Member, IEEE,* Zhenbin Zhang, *Senior Member, IEEE,* Yongchang Zhang, *Senior Member, IEEE,* Margarita Norambuena, *Member, IEEE,* Ali Emadi, *Fellow, IEEE,* Tobias Geyer, *Senior Member, IEEE,* Ralph Kennel, *Senior Member, IEEE,* Tomislav Dragicevic, *Senior Member, IEEE,* Davood A. Khaburi, Zhen Zhang, *Senior Member, IEEE,* Mohamed Abdelrahem, *Senior Member, IEEE,* Nenad Mijatovic, *Member, IEEE.*

Manuscript received January 2, 2021; revised March 27, 2021; accepted September 24, 2021. This work was supported in part by: ANID through projects Fondecyt 11180235, 1210208, 11190852, FB0008 and Anillo Project ACT192013; SERC Chile (CONICYT/FONDAP/15110019); National Natural Science Funds of China under Grant 51877207; the Australian Government through the Australian Research Council (Discovery Project No. DP210101382). (Corresponding author: Cristian Garcia)

J. Rodriguez, F. Flores-Bahamonde and L. Tarisciotti are with the Department of Engineering Sciences, Universidad Andres Bello, Santiago, 30332 Chile (e-mail: jose.rodriguez; freddy.flores; luca.tarisciotti@unab.cl).

C. Garcia is with the Department of Electrical Engineering, Universidad de Talca, Curico, 3340000 Chile (e-mail: cristian.garcia@utalca.cl).

A. Mora and M. Norambuena are with the Department of Electrical Engineering, Universidad Tecnica Federico Santa Maria, Valparaiso, 30332 Chile (e-mail: andres.mora; margarita.norambuena@usm.cl).

A. Davari is with the Faculty of Electrical Engineering, Shahid Rajaee Teacher Training University, Tehran 16788 15811, Iran (e-mail: davari@sru.ac.ir).

J. Rodas is with the Laboratory of Power and Control Systems, Facultad de Ingeniería, Universidad Nacional de Asunción, Paraguay (e-mail:jrodas@ing.una.py).

D. Valencia and A. Emadi are with the McMaster Automotive Resource Centre (MARC), McMaster University, Hamilton, Ontario L8P 0A6, Canada (e-mail: valend1; emadi@mcmaster.ca).

Mahmoud F. Elmorshedy is with the Department of Electrical Power and Machines Engineering, Faculty of Engineering, Tanta University, Tanta, 31521, Egypt (e-mail: Mahmoud.elmorshedy@f-eng.tanta.edu.eg).

F. Wang is with Quanzhou Institute of Equipment Manufacturing, Haixi Institutes, Chinese Academy of Sciences, Jinjiang, 362200, China (e-mail: fengxiang.wang@fjirsm.ac.cn; zuokunkun17@mails.ucas.ac.cn).

K. Zou is with Quanzhou Institute of Equipment Manufacturing, Haixi Institutes, Chinese Academy of Sciences, Jinjiang, 362200, China and also with the Institute for Electrical Drive Systems and Power Electronics, Technical University of Munich (TUM), 80333 Munich, Germany (e-mail: kunkun.zuo@tum.de).

W. Xu is with the State Key Laboratory of Advanced Electromagnetic Engineering and Technology, School of Electrical and Electronic Engineering, Huazhong University of Science and Technology, Wuhan 430074, China (e-mail: weixu@hust.edu.cn).

Z. Zhang is with the School of Electrical Engineering, Shandong University, Jinan 250061, China (e-mail: zbz@sdu.edu.cn)

Y. Zhang is with School of Electrical and Electronic Engineering, North China Electric Power University, Beijing 102206, China (e-mail: yozhang@ieee.org).

T. Geyer is with the ABB System Drives, 5300 Turgi, Switzerland (e- mail: t.geyer@ieee.org).

R. Kennel is with the Institute for Electrical Drive Systems and Power Electronics, Technical University of Munich (TUM), 80333 Munich, Germany (e-mail: ralph.kennel@tum.de).

***Abstract*—This paper presents the application of Model Predictive Control (MPC) in high-performance drives. A wide variety of machines have been considered: induction machines, synchronous machines, linear motors, switched reluctance motors, and multiphase machines. The control of these machines has been done by introducing minor and easy-to-understand modifications to the basic predictive control concept, showing the high flexibility and simplicity of the strategy. The second part of the paper is dedicated to the performance comparison of MPC with classical control techniques such as field-oriented control and direct torque control. The comparison considers the dynamic behavior of the drive and steady-state performance metrics such as inverter losses, current distortion in the motor, and acoustic noise. The main conclusion is that MPC is very competitive concerning classic control methods by reducing the inverter losses and the current distortion with comparable acoustic noise.**

***Index Terms*—Predictive control, variable speed drives, electric machine.**

I. INTRODUCTION

With the advances of electromobility, the control of electrical machines, a traditional research area, is now more active than ever [1]–[3]. Applications of controlled electrical motors in cars, trucks, buses, trains, scooters and bicycles are intensively investigated [4]–[11]. Different types of motors are being studied for these applications: Induction Machines (IM), Permanent Magnet Synchronous Machines (PMSM), Switched Reluctance Machines (SRM) to mention a few [5], [12]–[14].

T. Dragicevic and N. Mijatovic are with the Department of Electrical Engineering, Technical University of Denmark, 2800 Lyngby, Denmark (e-mail: tomdr; nm@elektro.dtu.dk).

D. A. Khaburi is with the Department of Electrical Engineering, Iran University of Science and Technology, Tehran 1311416846, Iran (e-mail: khaburi@iust.ac.ir).

Z. Zhang is with School of Electrical and Information Engineering, Tianjin University 92 Weijin Road, Nankai District, Tianjin 300072, Tianjin, China (e-mail: zhangz@tju.edu.cn).

M. Abdelrahem is with the Institute for Electrical Drive Systems and Power Electronics, Technical University of Munich (TUM), 80333 Munich, Germany and also with the Electrical Engineering Department, Faculty of Engineering, Assiut University, 71516 Assiut, Egypt (e-mail: mohamed.abdelrahem@tum.de).

Today, the dominant strategy for the control of electrical motors in electromobility is Field Oriented Control (FOC). This technique was invented 50 years ago at a time where microprocessors were not available [15], [16]. Using microprocessors this technique constantly has been improved and today is the standard for high performance drives.

The tremendous calculation power of modern microprocessors available today has motivated the investigation of different control techniques for high performance drives, with Model Predictive Control (MPC) being one of them. MPC has emerged as a very attractive alternative for drives applications, because it adapts in a very natural way the discrete nature of the controller (the microprocessor) to the load, which is a system with a finite number of switching states generated by the inverter. Using MPC it is not necessary to linearize the equations of the machine, to design linear controllers and to use Pulse Width Modulation (PWM) [17]–[21]. Several works have been published, related to the use of MPC in electrical drives [22]–[27].

This paper presents a review of recent and relevant MPC strategies applied to different types of machines: induction motors, synchronous motors, switched reluctance motors, multiphase motors, and linear motors. This paper shows how MPC is adapted to fulfill the particular restrictions presented by each electric machine type.

Aiming to be accepted by the industry, MPC techniques must demonstrate superior performance compared to existing high-performance strategies: FOC and Direct Torque Control (DTC). For doing so, the second part of this review paper is dedicated to assessing the performance of these control techniques. The main comparison criteria evaluate the dynamic behavior of electromagnetic torque. The assessment also considers steady-state performance metrics such as switching losses in the inverter, the ripple in the motor current, and the motor's acoustic noise, which is relevant for car applications.

The paper is organized as follows. Section II presents a short review of the main model predictive control strategies. Sections III, IV, and V present the main features related to the application of MPC in switched reluctance, linear induction, and multiphase machines, respectively. Section VI compares a model predictive torque control (MPTC) strategy based on Finite Control Set MPC (FCS-MPC) with the two most important high-performance control strategies used in industry, namely: FOC and DTC. The comparison evaluates the steady-state and dynamic performance. Section VII compares the technique called Model Predictive Pulse Pattern Control (MP^{3}C), [28]–[34] with standard control techniques, applied in a high power (>1MW) drive, using a 3-level Neutral Point Clamped (NPC) inverter. Section VIII compares the model predictive current control with linear current control and PWM for an electric car application, considering the losses of the inverter and acoustic noise [35]. Section IX presents the challenges and future works. Finally, section X presents the conclusions.

II. Predictive Control Strategies for Drives

The predictive control method includes different sub-branches, i.e., hysteresis-based control, trajectory-based control, deadbeat control, and MPC [36] [37]. The hysteresis control theory, which is also known as bang-bang control theory, was firstly introduced for predictive current control in [38]. The trajectory control method is based on forcing the variables of the system to track a predefined trajectory. Direct self control [39] and direct mean torque [40] are the most important methods in this category [41]. The combination of the hysteresis-based control and the trajectory-based control has become an independent family in the drive applications known as the Direct Toque Control [42]. This method showed that the predictive control is capable of the direct control of the desired variables like the torque and the flux [41]. Except for the DTC strategy, today two successful categories of the predictive control family in drive applications are deadbeat control, and MPC. These two categories were widely investigated for the drive applications during the last decade. The MPC method has been applied by two approaches, i.e., Continuous Control Set MPC (CCS-MPC) and FCS-MPC.

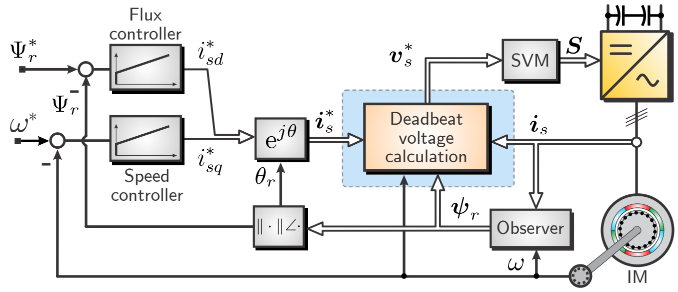

Fig. 1: Deadbeat-based FOC method.

A. Deadbeat Control in Drive Applications

The idea of the deadbeat control is based on calculation and application of the voltage vector that will move the operating point of the motor exactly to the desired torque and the flux [43]. The deadbeat method has been applied to drive applications because of the capability of a very fast dynamic response [44] and an accurate steady state response [43]. Fig. 1 shows a typical block diagram of the deadbeat control method for motor drives in field coordinates. The following equation shows the voltage reference calculation in deadbeat control of the induction motor [45]:

$$\boldsymbol{v}_s^* = \frac{\sigma L_s}{T_s}\left(\boldsymbol{i}_s^* - \boldsymbol{i}_s^k\right) + R_\sigma \boldsymbol{i}_s^k + \frac{k_r}{\tau_r}\left(j\omega\tau_r - 1\right)\boldsymbol{\psi}_r^k. \quad (1)$$

where $\tau_r = \frac{L_r}{R_r}$, $k_r = \frac{L_m}{L_r}$, $R_\sigma = R_s + k_r^2 R_r$, $\sigma = 1 - \frac{L_m^2}{L_s L_r}$, and T_s is the sampling period.

Despite the mentioned advantages of this technique, it shows a high sensitivity to different kinds of disturbances in practice. Most of the studies about the deadbeat method during the last decade are dedicated to robustness improvement. The research on this issue can be categorized as follows:

- Disturbance estimation and cancellation.
- Controller bandwidth tuning.
- Online parameter identification.
- Prediction model robustness improvement.

The disturbance estimators are used to estimate the general errors produced by system's the disturbances [46]. The estimated disturbance should be subtracted by the control law, which is the stator voltage reference. In [47], an ultra-local model is used to observe the system's disturbance. A combination of disturbance and load observers is proposed as the parallel-observer in [48].

Another technique to increase the deadbeat method's robustness to reduce the controller bandwidth was introduced in [44]. The bandwidth reduction of the controller is performed by dividing the error by two [48]. Through this technique, the tolerance of the parameters can be increased up to 200% while decreasing the deadbeat controlled system's dynamic performance.

The adaptive online parameter identification has been widely utilized to improve the robustness of the deadbeat method [43]. A Model Reference Adaptive System (MRAS) observer is used in [49] to adapt the speed and stator resistance simultaneously. The results of this study showed that a 150% uncertainty of the stator resistance is tolerated. However, the drift error is a common problem among MRAS-based observers. In [43], the estimation is performed one step ahead to reduce the drift error.

The closed-loop Luenberger prediction model has been introduced as the robust prediction model [50]. The feedback gains are calculated based on the H_∞ robust design. Though this method increases the robustness, it is proved that the method is not robust at near-zero speed region. In [51], [52], an integrator is used in the control loop to reduce the sensitivity and modify the dynamic response of the system.

Overall, the deadbeat control method is considered the faster control method in the predictive control family. Consequently, the sensitivity to parameters mismatch and estimation of disturbances are the main issues to overcome about this control method to achieve a high-performance motor drive controller.

B. Continuous Control Set MPC (CCS-MPC)

This control strategy was first introduced as the generalized predictive control [53] and it is considered the basic form of MPC. As shown in Fig. 2, this control method employs carrier-based PWM such as Sinusoidal PWM (SPMW) or Space Vector Modulation (SVM) and it is also referred to as Indirect MPC [37].

This control method computes the voltage reference by minimizing a given cost function, representing the tracking error of the controlled variables. The cost function for current control considering a prediction horizon of one step is defined as below [54]:

$$g = \left(i_{sd}^{*} - i_{sd}^{k+1}\right)^2 + \left(i_{sq}^{*} - i_{sq}^{k+1}\right)^2. \tag{2}$$

Suppose both the constraints related to the feasibility region in which the voltage vector belongs (input constraints) and the current limits (state constraints) are not considered. In that case, an unconstrained Quadratic Programming (QP) is established, and the voltage vector can be easily obtained by

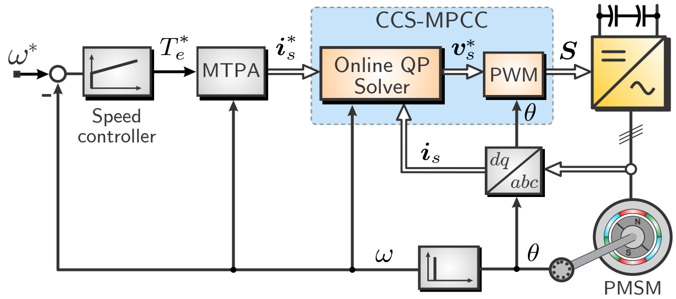

Fig. 2: CCS-MPC-based MPTC for PMSMs.

solving $\nabla g = 0$. For instance, if a surface-mount PMSM is utilized, the optimized voltage variables v_{sd}^k and v_{sq}^k are:

$$v_{sd}^k = \frac{L_s}{T_s}(i_{sd}^* - i_{sd}^k) + R_s i_{sd}^k - L_s \omega^k i_{sq}^k, \tag{3a}$$

$$v_{sq}^k = \frac{L_s}{T_s}(i_{sq}^* - i_{sq}^k) + R_s i_{sq}^k + L_s \omega^k i_{sd}^k + \omega^k \psi_{\mathrm{pm}}. \tag{3b}$$

The studies in [54]–[56] show that the CCS-MPC results in a low ripple for the torque and the current of the machine. Also, the computational burden of this control method is low. However, as shown in (3), the performance of the controller would be deteriorated by the parameter variations (including stator resistance, stator inductance, and permanent magnet flux linkage) and nonlinearity. Thus, the sensitivity of the method is high, similar to the deadbeat control strategy.

To overcome this issue, many approaches have been proposed in the literature. For instance, as indicated in [37], the robustness of the Indirect MPC is improved by penalizing the control effort[1] in the cost function allowing for less aggressive control actions. In [54], a disturbance observer is applied to reduce the sensitivity of the method. Besides, the rotor position is eliminated from the prediction model in [56] to increase the robustness of the sensorless motor drive.

Furthermore, when input and/or state constraints are considered for the MPC formulation [37], then either efficient QP solvers can be employed (e.g., interior-point, active-set methods [57]), or the unconstrained solution can be projected onto the feasible set. In [58], a CCS-MPC strategy with input and state constraints was introduced for MPTC in PMSMs, in which an active-set algorithm to solve efficiently the associated QP problem is implemented in a low-cost control platform.

C. Finite Control Set MPC (FCS-MPC)

The distinguishing point of this MPC approach is the consideration of the finite nature of the power converter. Considering this feature, the FCS-MPC predicts the behaviour of the variable to be controlled for a set of admissible switching positions. The cost function should be examined for all feasible voltage vectors, and the optimum switching state is the one minimizing the cost function. For instance, if a traditional two-level inverter is utilized and a prediction horizon of one step

[1] In CCS-MPC, the control effort stands for change in the voltage vector or change in the modulation index. In the context of FCS-MPC, the control effort concept refers to the switching effort and penalizes the number of commutations of the power semiconductors.

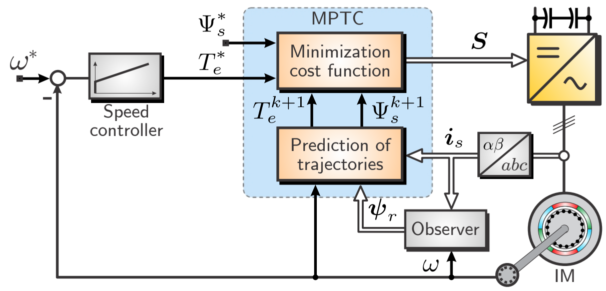

Fig. 3: FCS-MPC-based MPDT for IMs.

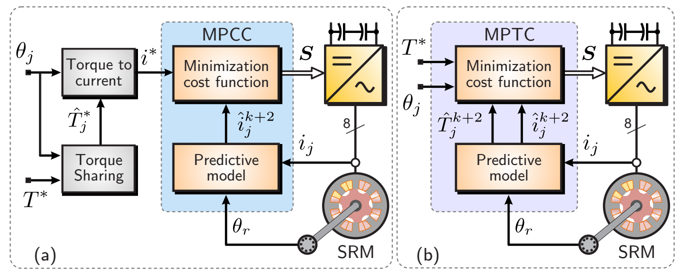

Fig. 4: Block diagram for control algorithms in SRM drives (a) Current reference generated with offline torque sharing technique and MPCC for phase current tracking (b) MPTC.

is considered, the cost function should be evaluated for the set of possible voltage vectors [59]–[61].

The block diagram of the FCS-MPC method applied for model predictive torque control is illustrated in Fig. 3. As indicated above, the stator flux and electromagnetic torque of the IM can be predicted by using [62]:

$$\boldsymbol{\psi}_s^{k+1} = \sigma L_s \boldsymbol{i}_s^{k+1} + k_r \boldsymbol{\psi}_r^{k+1} \tag{4a}$$

$$T_e^{k+1} = \frac{3}{2} \boldsymbol{\psi}_s^{k+1} \times \boldsymbol{i}_s^{k+1} \tag{4b}$$

In (4), the future trajectories for the stator current $\boldsymbol{i}_s^{k+1}$ and rotor flux $\boldsymbol{\psi}_r^{k+1}$ are obtained from the following discrete-time model:

$$\begin{bmatrix} \boldsymbol{i}_s^{k+1} \\ \boldsymbol{\psi}_r^{k+1} \end{bmatrix} = \begin{bmatrix} 1-\frac{T_s R_\sigma}{\sigma L_s} & \frac{T_s k_r}{\sigma L_s}\left(\frac{1}{\tau_r}-j\omega^k\right) \\ \frac{T_s L_m}{\tau_r} & 1-T_s\left(\frac{1}{\tau_r}-j\omega^k\right) \end{bmatrix} \begin{bmatrix} \boldsymbol{i}_s^k \\ \boldsymbol{\psi}_r^k \end{bmatrix} + \begin{bmatrix} \frac{T_s}{\sigma L_s} \\ 0 \end{bmatrix} \boldsymbol{v}_s^k \tag{5}$$

The cost function for controlling the torque and stator flux magnitude is:

$$g_j = \left(T_e^* - T_{ej}^{k+1}\right)^2 + \lambda_\Psi \left(\Psi_s^* - \Psi_{sj}^{k+1}\right)^2. \tag{6}$$

Consequently, the cost function (6) should be computed for all possible voltage vectors according to the FCS-MPC working principle, where λ_Ψ is the flux weighting factor. Then, the inverter applies the voltage vector that minimizes the cost function. This process is repeated each control interval T_s.

The advantages of the FCS-MPC can be summarized as below [61]–[65]:

- It is straightforward to include nonlinearities, constraints, and variables of different nature in the optimization problem.
- There is no need for a modulator which is useful when a multi-level or a matrix converter is applied.
- The dynamic performance of the control method is faster than the one obtained with FOC.

Despite the mentioned advantages, there are some drawbacks with the FCS-MPC method. The first problem is the weighting factor in the cost function which is the common problem of all cost function based model predictive control methods [66]. Generally, four techniques have been applied for this problem.

- Finding the optimum weighting factors [67].
- Simplified FCS-MPC [68].
- Decision making based methods [69].
- Sequential FCS-MPC [70].

The second drawback of the FCS-MPC is the high ripple for the torque and the current. A promising solution to mitigate these issues is the so-called modulated MPC strategy introduced in [71], [72] for PMSMs. Similar to the modulated MPC, a control strategy that manipulates the switching states and their application times aiming to control the stator flux trajectory is proposed in [73] to improve the overall performance of IM-based drives.

The last problem of FCS-MPC is the high computational burden when it is adapted for multilevel converter applications. Voltage vector elimination has been utilized in [74] aiming to reduce the number of possible vectors that should be calculated.

III. Application of FCS-MPC in Switched Reluctance Machine (SRM)

SRMs, magnet-free and double salient pole structure offer a simpler construction and robust high-speed and high-temperature operation [75], making them interesting for reliable fault-tolerant operation [76]. These features have found a suitable position in applications such as vacuum cleaners, jack hammers, compressors, and electric vehicle systems [77], [78]. Although SRMs are candidates for high-performance and safety-critical systems such as automotive traction or aerospace [79], [80], in practice, they have not seen such scenarios due to their inherent torque ripple and acoustic noise [81].

Several design considerations have been proposed and comprehensively reviewed in [82]–[84]. However, torque control is not as straightforward as it is in conventional AC drives. The highly nonlinear torque-current-position relation requires the definition of torque sharing rules that are mapped as phase reference currents through lookup tables [85], in a similar way as FOC. Some of these rules include Torque Sharing Functions (TSFs) [86] or Radial Force Shaping (RFS) algorithms [87]. Nevertheless, the current tracking is a challenging task in such a nonlinear machine. This high complexity has become an interesting target for MPC to handle.

1) MPC of SRM drives: There are two alternative implementations of MPC in SRM, as shown in Fig. 4. The first one, in Fig. 4(a), emulates the FOC obtaining reference currents from pre-calculated lookup tables. A Model Predictive Current

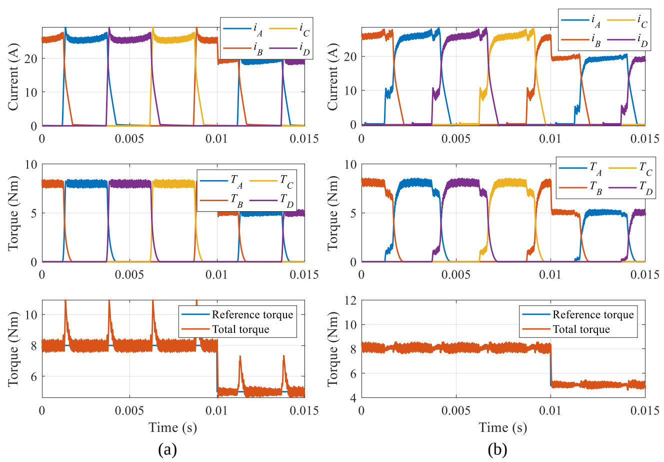

Fig. 5: Results for torque tracking at 1000 rpm of a four-phase 8/6 SRM using (a) TSF and MPCC (b) MPTC.

Control (MPCC) algorithm tracks the phase currents based on the discrete machine flux equation as [88],

$$\psi_j^{k+1} = \psi_j^k(i_j^k, \theta_j) + T_s(v_j^k - R_j i_j^k), \tag{7}$$

where v_j, i_j, R_j, L_j and ψ_j are the voltage, current, resistance, and flux linkage of the phase j, respectively. Notice that the dependence of the flux linkage on both the current and electrical angle θ_j is highly nonlinear; therefore, the predictive model usually relies either on approximated analytical equations or static maps [89]. In the latest, ψ_j^k is obtained from the static characteristics $\psi(i, \theta)$ as a lookup table. The predicted ψ_j^{k+1} is used to obtain i_j^{k+1} using a second lookup table $i(\psi, \theta)$. In practice, this prediction uses on ψ_j^{k+2} for delay compensation. Alternatively, Fig. 4(b) uses a MPTC approach, which generates a switching pattern with the comparison of the reference torque and the predicted torque from the predictive model [90]. The main advantage is the online definition of torque sharing laws. The torque T_{ej}^{k+1} is predicted from the phase torque T_{ej}^{k+1} and i_j^{k+1} as,

$$T_e^{k+1} = \sum_{j=1}^{m} T_{ej}^{k+1}\left(i_j^{k+1}, \theta_j^{k+1}\right). \tag{8}$$

2) Cost functions: The current tracking can be defined with eq. (9a) [91]. As the SRMs commonly use asymmetric converters, there are three possible switching states per phase. For a four-phase SRM it means $3^4 = 81$ possible combinations. Assuming no more than two phases simultaneously active, it is reduced to 9 possible states [88]. For the MPTC approach, (9b) can be adopted [90], [92]. It is common to include a term to penalize the phase currents to obtain the reference torque with the minimum conduction losses [93]. The cost functions in (9) evaluate the possible switching states to obtain the S_{opt}^{k+2} that minimizes the error. Fig. 5 shows the phase currents, phase torque and total torque for the algorithms shown in Fig. 4. MPCC guarantees a proper current regulations with minimum ripple, but the algorithm, in this case TSF, fails to reduce torque ripple requiring additional improvement. MPTC, contrarily, provides a smooth torque sharing with more diverse current waveforms, thus evidencing the flexibility of MPCC.

$$g_i = \left(i^* - {i_j}^{k+2}\right)^2, \tag{9a}$$

$$g_{T_e} = \left(T_e^* - T_{ej}^{k+2}\right)^2 + \sigma_i \sum i_j. \tag{9b}$$

3) Particular considerations and constrains: SRM control usually rely on Finite Element Analysis (FEA) models to obtain the static maps, which possibly makes the parameter variations considerable. Solutions have been proposed like online parameter estimation to compensate for variations in the phase inductance and filtering techniques for measurement inaccuracies [94]. MPC for SRM is still at an early stage, and further work on secondary objectives such as acoustic noise and fault-tolerance is still required.

IV. Application of FCS-MPC in Linear Induction Machine

Linear Induction Machines (LIMs) have many applications such as reciprocating compressor, packing materials handling and also it is used in subway systems in various countries such as the USA, Japan, and China [95]–[97]. Despite comprehensive research of MPC for conventional rotating machines presented in [95], [98], few works have focused on MPC for LIM applications. Different MPC strategies have been presented for LIM applications [98]–[106]. Some of these strategies have focused on the reduction of thrust and primary flux-linkage ripples, the decreasing distortion of the primary current, achieving the Maximum Thrust Per Ampere (MThPA), and eliminating the weighting factor from the cost function.

In [99], both running and safety operation for the LIM have been improved by applying Multistep Model Predictive Control (MMPC). Meanwhile, the development of two or three voltage vectors has been proposed in [100], [101] so as to reduce the current ripples. In [100], the armature current has been limited within a safe region by inserting a penalty over-current factor in the designed cost function. Moreover, an improved deadbeat control with an iterative algorithm is proposed in [101] to solve the problem of current and voltage constraints in the traditional DBC. In addition, the deadbeat control has been improved by producing the maximum thrust in the whole working condition [102]. Further, the FCS-MPC is improved by adding the MThPA criteria with different condition such as presented in [103]–[105]. Finally, some researchers have developed the MPC without weighting factor to reduce the time consumed like [98], [106].

In order to completely eliminate the weighting factors, reduce the calculation process and improve the performance of the LIM drive system, a new cost function is proposed in [103]. The new cost function is based only on the primary flux-linkage error. Extra improvement can be accomplished with the proposed control approach by achieving MThPA criterion. This method is called Finite-Set Model Predictive Direct Flux Control (FS-MPDFC).

Based on the dynamic model of the LIM, the error between the reference thrust and the actual thrust $\Delta F_e = F_e^* - F_e$ can

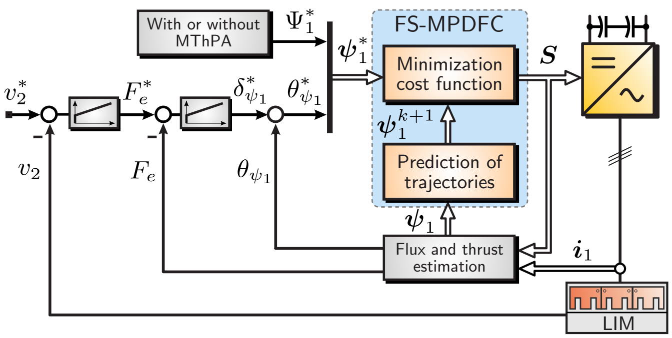

Fig. 6: The proposed MThPA based the FS-MPDFC for LIM drive system.

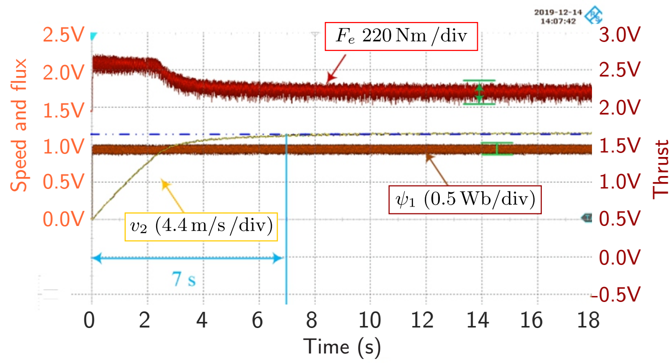

Fig. 7: Responses of thrust, primary flux-linkage, and linear speed for LIM based on FS-MPDFC.

be expressed by [105],

$$\Delta F_e = \frac{3}{2}\frac{\pi}{\tau}\frac{1}{\tau_l \sigma}\|\boldsymbol{\psi}_1\|\|\boldsymbol{\psi}_2\|\big(\sin(\theta_{12}+\delta_{\psi 1})-\sin(\theta_{12})\big), \quad (10)$$

where θ_{12} is the angle between the primary and secondary flux-linkages. Notice that, from (10), the relation between the thrust error and the incremental deviation of the thrust angle, $\delta_{\psi 1}$ is non-linear. Therefore, a PI controller is used to generate the incremental variation of the thrust angle. Hence, the reference primary flux-linkage can be calculated by,

$$\psi_{1\alpha}^* = \|\boldsymbol{\psi}_1^*\|\cos(\theta_{\Psi_1}+\delta_{\psi_1}) \quad (11)$$
$$\psi_{1\beta}^* = \|\boldsymbol{\psi}_1^*\|\sin(\theta_{\Psi_1}+\delta_{\psi_1}), \quad (12)$$

where $|\boldsymbol{\psi}_1^*|$ is the amplitude of reference primary flux-linkage, and $\theta_{\Psi 1}$ the angle of the estimated primary flux linkage. In order to guarantee the maximal thrust, the reference primary flux-linkage $|\boldsymbol{\psi}_1^*|$ can be calculated based on [103].

The proposed cost function depends only upon $\boldsymbol{\psi}_{\alpha\beta}$ reference and predicted components as expressed by

$$g = \left(\psi_{1\alpha}^* - \psi_{1\alpha,i}\right)^2 + \left(\psi_{1\beta}^* - \psi_{1\beta,i}\right)^2. \quad (13)$$

The block diagram of the proposed FS-MPDFC strategy is shown in Fig. 6. The final expression of the predicted primary flux-linkage can be written as:

$$\psi_{1\alpha,i}(k+1) = \psi_{1\alpha}(k) + T_s(u_{1\alpha,i}(k) - R_1 i_{1\alpha}(k)) \quad (14)$$
$$\psi_{1\beta,i}(k+1) = \psi_{1\beta}(k) + T_s(u_{1\beta,i}(k) - R_1 i_{1\beta}(k)). \quad (15)$$

The proposed FS-MPDFC is tested under the thrust load of 100 N, linear speed of 6 m/s and sample time of $2\cdot10^{-4}$s. The responses of electromagnetic thrust, primary flux linkage, and linear speed are shown in Fig. 7. It is observed that the FS-MPDFC can achieve faster response with lower thrust ripple compared to the other FS-MPDTC method mentioned in [103].

V. Application of FCS-MPC in Multiphase Machine

Multiphase systems are those that have more than three phases ($n = 5, 6, 7, 9, 12, \ldots$) and could be of either induction or synchronous type. The possibility to split the power into more phases and its inherent fault-tolerance operation with no extra hardware are the main advantages compared with traditional three-phase systems [107]. For that reasons, multiphase systems are considered ideal for fault-tolerant and high-power applications such as electric propulsion and traction (i.e. ships and electric vehicles) and generation systems (i.e. offshore wind energy systems) [108]. Nevertheless, the additional degrees of freedom (typically named $x-y$ planes) that exist in multiphase systems also make them a good alternative for various nontraditional purposes such as battery chargers for electric vehicles or multimotor systems fed by a single power converter [109].

The application of new control techniques for multiphase systems has been undoubtedly one of the main research topics that has caught the attention of the MPC community. Therefore, much effort has been directed over the last decade to improve the performance of traditional control schemes by using MPC-based controllers. The application of FCS-MPC as a MPCC for multiphase machines is presented below, taking a 6-phase IM as an illustrative example.

A. Standard MPCC of Multiphase Machines

Fig. 8 shows the control structure of a 6-phase IM variable speed drive using the standard Indirect Rotor Field-Oriented Control (IRFOC) technique where the inner current control loop is implemented with the standard MPCC. Then, the stator current reference in the $\alpha-\beta$ plane ($\boldsymbol{i}_{s,\alpha\beta}^*$) is generated from the outer speed control loop and from the d-axis current reference (i_{sd}^*). The MPCC uses the following discrete-time model of the system to predict the future values of the 6-phase IM's currents $\boldsymbol{i}_m = \left[\boldsymbol{i}_{s,\alpha\beta}^T\,\boldsymbol{i}_{s,xy}^T\,\boldsymbol{i}_{r,\alpha\beta}^T\right]^T$:

$$\boldsymbol{i}_m^{k+1} = \boldsymbol{A}^k\boldsymbol{i}_m^k + \boldsymbol{B}\boldsymbol{v}_s^k, \quad (16)$$

where $\boldsymbol{i}_{s,\alpha\beta} = \left[i_{s\alpha}\,i_{s\beta}\right]^T$ and $\boldsymbol{i}_{s,xy} = \left[i_{sx}\,i_{sy}\right]^T$ denote the stator current in the $\alpha-\beta$ and $x-y$ planes, respectively. The rotor current is defined accordingly $\boldsymbol{i}_{r,\alpha\beta} = \left[i_{r\alpha}\,i_{r\beta}\right]^T$. Matrices $\boldsymbol{A}^k$ and $\boldsymbol{B}$ depend on the 6-phase IM parameters and the present value of both, the rotor speed ω^k and the sampling time T_s. The input stator voltages are denoted by $\boldsymbol{v}_s=\left[\boldsymbol{v}_{s,\alpha\beta}^T\,\boldsymbol{v}_{s,xy}^T\right]^T$. To provide delay compensation, a two-step ahead prediction of the stator currents $\boldsymbol{i}_s=\left[\boldsymbol{i}_{s,\alpha\beta}^T\,\boldsymbol{i}_{s,xy}^T\right]^T$ is typically performed. To this end, it is necessary to estimate and predict the unmeasurable rotor currents at instant $k+1$ [110], [111].

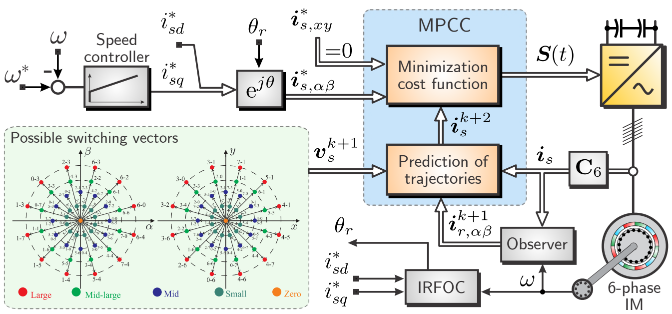

Fig. 8: Voltage space vectors and 64 switching states in $\alpha-\beta$ and $x-y$ planes and MPCC scheme for a 6-phase IM.

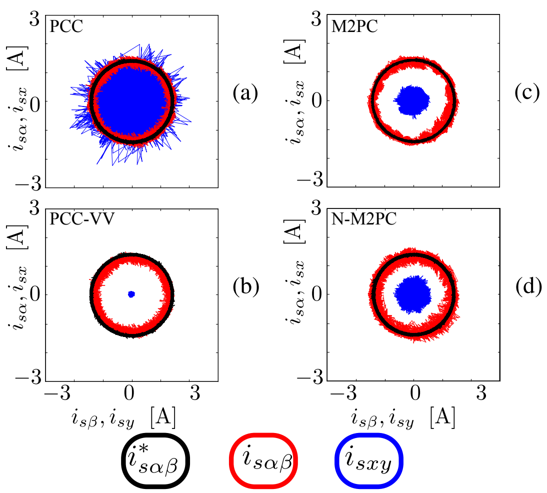

Fig. 9: Experimental stator current responses presented in [112] using (a) standard MPCC; (b) MPCC-VV; (c) M2PC; (d) N-M2PC control methods. The same stator current references are applied for all controllers (Reproduced from [112]).

The cost function (17) is used to define the desired behavior, i.e. the stator current tracking. For a 6-phase IM, the cost function is evaluated 49 times, and then, the Voltage Source Inverter (VSI) switching state (S_{opt}^{k+2}) for the stator voltage vector that minimizes the cost function is selected and applied to the 6-phase IM by means of the VSI during the next sample time.

$$g = \left\| \boldsymbol{i}_{s\alpha\beta}^{*k+2} - \boldsymbol{i}_{s\alpha\beta}^{k+2} \right\|_2^2 + \lambda_{xy} \left\| \boldsymbol{i}_{sxy}^{*k+2} - \boldsymbol{i}_{sxy}^{k+2} \right\|_2^2. \qquad (17)$$

The tuning of the weighting factor (λ_{xy}) is a heuristic procedure providing trade-off between the variables of interest [113]. Other examples of cost functions for multiphase machines include reduction of common-mode voltages, torque ripple minimization and VSI switching losses [114], [115].

B. Particular Considerations and Constraints

The standard MPCC is an alternative to the inner PI current controller used in typical FOC schemes. The latter technique is one of the most used control structures for multiphase machines. Compared to the standard PI current controller, MPCC provides faster current tracking and wider current control bandwidth at the expense of a higher computational cost, worse $x-y$ current control, and higher current ripple. An open issue is the simultaneous control of primary $\alpha-\beta$ flux/torque production plane and secondary $x-y$ machine losses plane. Many variations of the standard PCC have been proposed for this problem. Fig. 9 summarizes the experimental results for some of the most recent variations of the MPCC method, namely the MPCC with Virtual Vector (MPCC-VV) [116], Modulated Model Predictive Control (M2PC) [117] and a novel variation named N-M2PC [112]. The most recent reviews of PCC structures with different cost functions for 5-phase IM and 6-phase IM are available in [118] and [119], respectively.

TABLE I: Control algorithms comparison

	FOC	DTC	MPTC
Tuned Param.	6	4	3
Exter. Control	PI	PI	PI
Inner Control	2 PI	2 Hys. Contr.	Pred. Contr.
Flux Angle	Yes	Yes	No
Coordinate Transf.	Yes	No	No
PWM	Yes	No	No
Constraints inclusion	Difficult	Difficult	Easy
Control Complex.	High	High	Low
Computational Burden	8 μs	8 μs	12 μs

VI. General Assessment of FCS-MPC with High Performance Control Strategies

From the theoretical point of view [120]–[122], the comparison of FOC, DTC and MPTC (see Fig. 3) is summarized in Table I, including the required tuned parameters, external loop controller, inner loop controller, system control, etc. In this section, these methods are studied comparatively by using experimental tests.

A. Evaluation Criteria

1) Switching frequency: Unlike the FOC method, where the carrier frequency f_c of the PWM imposes the switching frequency as $f_{\text{sw}} = f_c/2$, the DTC and MPTC strategies perform variable switching frequency. Thus, to ensure a fair

TABLE II: Parameters of the IM

Parameter		Value
dc-link voltage	V_{dc}	582 V
Stator resistance	R_s	2.68 Ω
Rotor resistance	R_r	2.13 Ω
Mutual inductance	L_m	275.1 mH
Stator inductance	L_s	283.4 mH
Rotor inductance	L_r	283.4 mH
Nominal Speed	ω_{nom}	2772 rpm
Nominal Torque	T_{nom}	7.5 Nm
Rotational inertia	J	0.005 kg/m^2

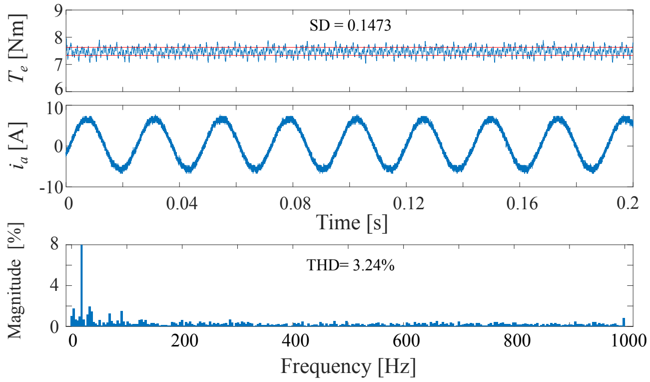

(a)

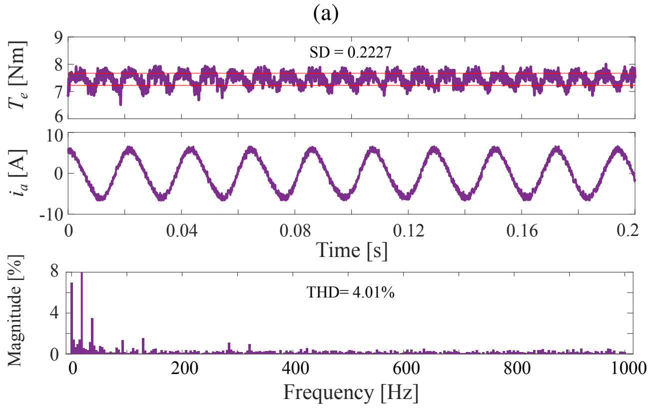

(b)

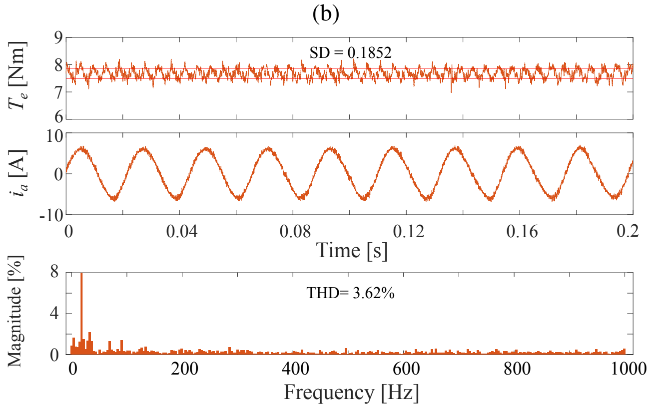

(c)

Fig. 10: Experimental results: steady-state performance under three control algorithms. (a) FOC; (b) DTC; and (c) MPTC.

comparison, the goal is to establish an average switching frequency equal to the one obtained using FOC. To this end, the DTC's switching frequency is taken as a reference to adjust the sampling frequency used in the MPTC and the PWM's carrier frequency employed in the FOC.

2) Steady-state performance: The Standard Deviation (SD) is used in this work to quantify the torque ripple. Besides, the current Total Harmonic Distortion (THD) is used to compare the performance of the tested control methods.

3) Dynamic performance: In this work, the time for the electromagnetic torque to reach the reference is used to evaluate all control algorithms' dynamic performance.

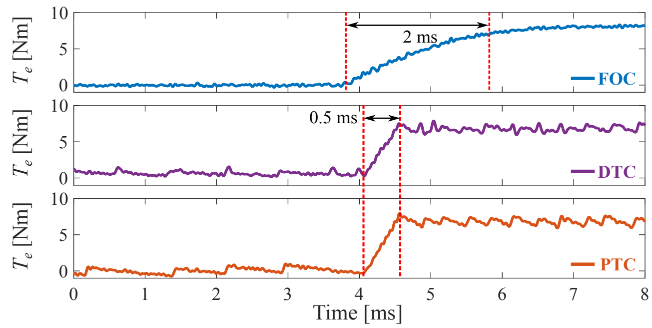

Fig. 11: Experimental results: dynamic torque response under three control algorithms.

B. Performance Evaluation

The IM test bench consists of two 2.2 kW squirrel-cage IM. The load machine is controlled by a 3.0 kW Danfoss VLT FC302 inverter to provide load torque, and the main machine is driven by a 14 kVA servostar600 inverter. The parameter of the IM are summarized in Table II. A self-made 1.4 GHz real-time computer system, Embedded PC104, is used for the control system of the inverter, with 16 kHz sampling frequency. All methods are carried out experimentally on the same test bench and using the same speed PI controller with 8 rad/s bandwidth.

To demonstrate the steady-state performance of all methods, the first comparative experiment is tested at full speed (2772 rpm) with a full load torque (7.5 Nm), as shown in Fig. 10. It should be noted that we have done a lot of experiments to tune the relevant parameters to achieve the optimal performance of each method. The measured THD of FOC, DTC and PTC are 3.2%, 4.0%, and 3.6%, respectively. It is clear that FOC algorithm achieves the best current performance at this operating point. FOC and PTC achieve smaller torque ripples, which are 0.8 Nm and 0.9 Nm, and the SD of torque are 0.1473 and 0.1852, respectively. DTC has slightly bigger ripples of 1.2 Nm, and the SD is 0.2227.

At the same time, when evaluating the error between the observed load reference value (7.5 Nm) and the torque fluctuation average value, only the FOC algorithm achieves a zero torque tracking error, which is due to the use of internal current PI controllers and the modulator. However, more PI parameters need to be tuned for a cascaded control structure.

Dynamic performance is one of the important indicators for evaluating various algorithms. Therefore, the torque dynamics of all methods are compared in the second test under the step-change load torque (from 0 Nm to 7.5 Nm), as shown in Fig. 11. From this picture, we can see that FOC algorithm takes a long time (2 ms) to reach the torque reference, because the inner current loop with limited bandwidth will limit the dynamics of the outer speed loop and the use of modulator will cause a delay. On the contrary, DTC and MPTC exhibit a shorter dynamic process (0.5 ms) because they have theoretically unlimited bandwidth. However, the primary disadvantage of the direct control method is that the selected voltage vector will be kept throughout the control interval, which possibly results in higher torque ripple.

To evaluate the dynamic performance over the entire speed

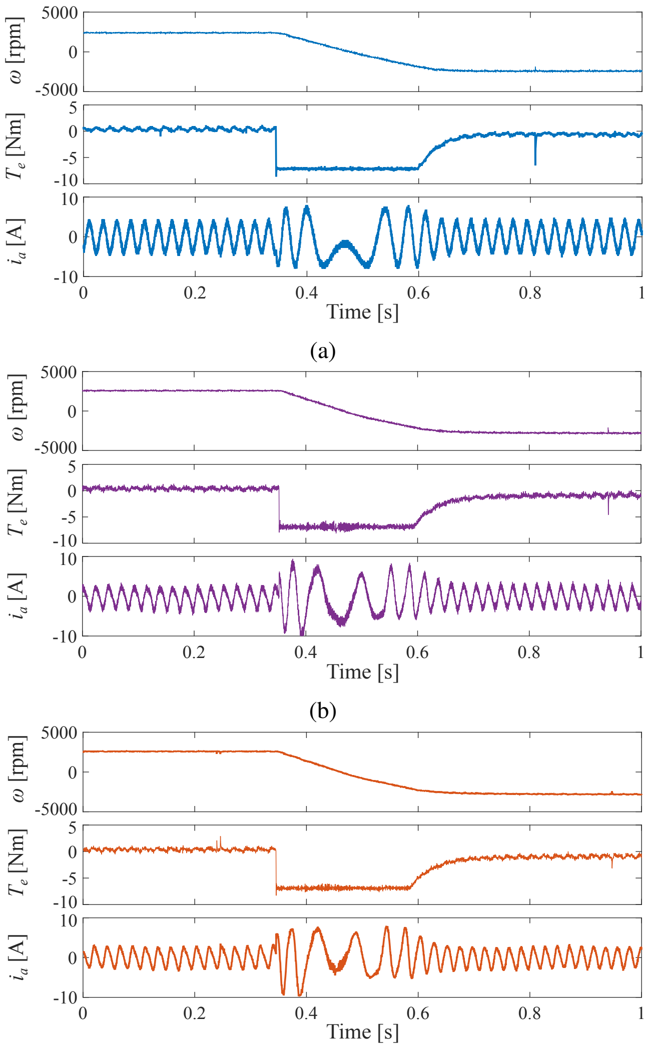

(a)

(b)

(c)

Fig. 12: Experimental results: reversal performance under three control algorithms. (a) FOC; (b) DTC; (c) MPTC.

range, the final comparative experiment demonstrates a full speed reverse test. Fig. 12 shows the results of rotating speed, electromagnetic torque, and stator current of all methods, respectively. As can be seen from the figure, all methods have achieved very similar results. While, FOC shows better current performance, which is the benefit of using the independent inner current PI controller. In the MPTC algorithm, the cost function considers the prediction errors of torque and flux. Therefore, the weighting factor determines the electromagnetic torque performance and the quality of magnetic flux. In summary, all methods in the comparison result can achieve acceptable control performance throughout the entire speed range.

Finally, the performance comparison of the tested control strategies in terms of switching frequency, current THD, torque SD, among other indexes, is summarized in Table III. As shown, the FOC algorithm's steady-state performance is better since, for similar switching frequencies, the current THD and torque ripple are slightly lower. However, in terms of

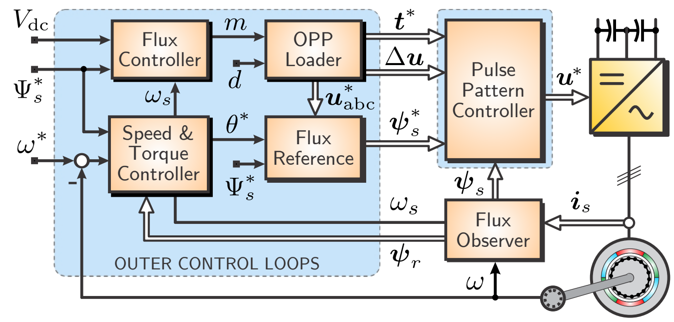

Fig. 13: MP^{3}C scheme based on optimized pulse patterns.

the dynamic performance, the FOC algorithm takes a longer settling time for torque transients when compared to MPTC and DTC strategies. Besides, MPTC can achieve dynamic responses like the DTC while keeping better steady-state performance.

VII. Assessment of MPC in a High Power Drive

A. MP^{3}C Control Strategy

The block diagram of the MP^{3}C strategy is depicted in Fig. 13. This controller combines the modulator and inner control loop in one computational stage using the receding horizon control policy [28]–[34]. From this perspective, for a given input trajectory, an internal model of the drive system allows predicting the system's output trajectory over a prediction horizon. An optimization stage minimizes the stator flux error by manipulating the time-instant of the optimal switching transitions derived from Optimum Pulse Patterns (OPP) [123].

B. Experimental Results

Experimental results for a medium-voltage NPC inverter (dc-link voltage is set to $V_{\mathrm{dc}} = 4.84$ kV) driving a 3.3 kV IM rated at 1140 kVA are summarized in this review paper (further details can be found in [33]).

Torque steps from 85% to 35% rated torque are shown in Fig. 14. MP^{3}C achieves the same torque settling time as DTC [124], [125], which is below 1 ms. This feature is due to the insertion of additional switching transitions into the switching pattern in case of large stator flux errors [30].

C. Assessment and Comparison with FOC-SVM

To quantify the user benefits of the MP^{3}C strategy in relation to the standard FOC with space vector modulation (SVM), a comprehensive simulation work of an idealized

TABLE III: Comparative analysis of experiments

	FOC	DTC	MPTC
Switching Freq.	4 kHz	4 kHz	3.92 kHz
Current THD	3.2%	4.0%	3.6%
Torque SD	0.1473	0.2227	0.1852
Dynamics	2 ms	0.5 ms	0.5 ms

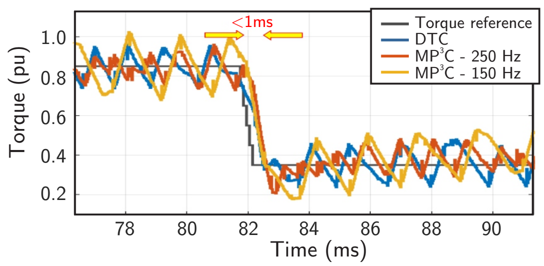

Fig. 14: Medium-voltage experimental results: MP^{3}C and DTC during a torque reference step from 85% to 35% rated torque, [33].

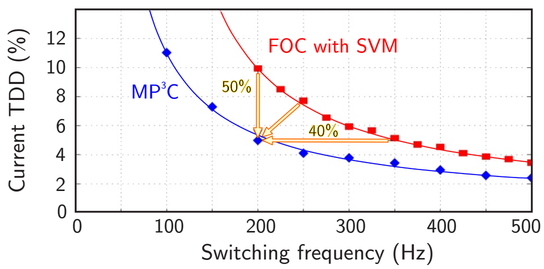

Fig. 15: Simulation results: current TDD vs switching frequency when comparing FOC-SVM and MP^{3}C (operating at full load), [33].

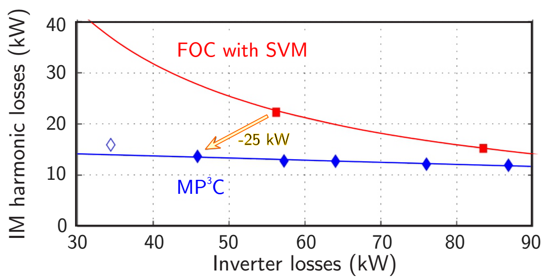

Fig. 16: Simulation results: Trade-off between the harmonic losses of the IM and the inverter losses, [33].

variable speed drive system was done in [33]. The harmonic performance of MP^{3}C with that of FOC-SVM is compared in Fig. 15. As shown, up to 50% lower current distortions or up to 40% lower switching frequency can be obtained by using MP^{3}C. A third alternative is to reduce both the switching frequency and the current distortions. An example of this approach is addressed by the diagonal arrow in Fig. 15. Here, MP^{3}C reduces the switching frequency by 20% and the current TDD by 35%.

As can be concluded from the above analysis, the performance of the drive system can be optimized by adequately reducing the iron and copper losses in the IM and the switching losses in the power converter. Also, low current distortions imply low ripple of the electromagnetic torque, which leads to lower mechanical stress. This feature allows improving the reliability and also enables increasing the maintenance intervals to reduce the operational costs of the drive system.

In an effort to quantify these benefits, detailed simulations of a 3.3 kV drive system with a 10.3 MW IM were carried

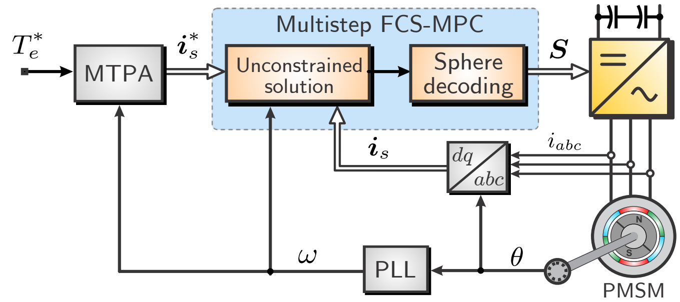

Fig. 17: Multistep model predictive current control for electrical car applications, [35].

out (further details in [33]). The trade-off between the inverter losses and the harmonic losses of the machine is shown in Fig. 16 when varying the switching frequency at nominal speed and load. It is clear from the results that MP^{3}C achieves a superior performance in terms of losses. As indicated by the arrow in Fig. 16, MP^{3}C at f_{sw}=150 Hz achieves a total loss reduction of 25 kW with respect to SVM at f_{sw}=250 Hz. This loss reduction can have a significant impact on both the capital expenditure as well as the operating costs of the system. For instance, by considering an electricity price of 80€ per MWh, the operational cost of the whole drive system can be reduced by 21k€ per year, [33].

VIII. Assessment of MPC for Electric Vehicles Application

The implementation of predictive control for a multi-step prediction, or also known as long-horizon prediction, has been proposed as a control strategy in power electronics, [126]. The main characteristics of this method is its ability to work with lower switching frequency, reducing the losses of the inverter in comparison with PWM [127]–[129]. This last characteristic has allowed it to position itself as an attractive strategy for electromobility applications, where energy efficiency is essential, [35]. Sphere decoding allows one to solve the underlying integer optimization problem in a computationally efficient way, [130], [131].

The proposed multi-step strategy with sphere decoding in [35] is shown in Fig. 17. The proposed method was implemented in a two-level VSI feeding a Interior-PMSM which is a typical electrical drive system for electrical car. In this work the cost function used is,

$$g = \sum_{k=t}^{t+N} (1-\lambda_u)\left\|\Delta \boldsymbol{i}_{dq}^{k+1}\right\|_2^2 + \lambda_u \left\|\Delta \boldsymbol{u}^k\right\|_2^2, \qquad (18)$$

where the control objectives are the direct and quadrature machine currents along with the change in the three-phase switching positions to minimize the commutations.

The efficiency in the use of energy is crucial today. This becomes even more important in electromobility applications where the available energy is limited, as is the case with an electric car. Fig. 18 shows the performance of multistep strategy, where it can be seen that it is possible to reduce the losses in the converter for the same harmonic distortion.

TABLE IV: Measurements showing the total inverter losses difference $\Delta P = 100 \times (P_{\text{MPC}} - P_{\text{FOC}})/P_{\text{FOC}}$.

Load Torque (Nm)	Speed (rpm) 1000	2000	3000	4000
10	-26%	-14%	-13%	-14%
20	-20%	-9%	-9%	-13%
30	-16%	-6%	-7%	-12%
40	-10%	-5%	-6%	-11%
50	-7%	-4%	-6%	-10%

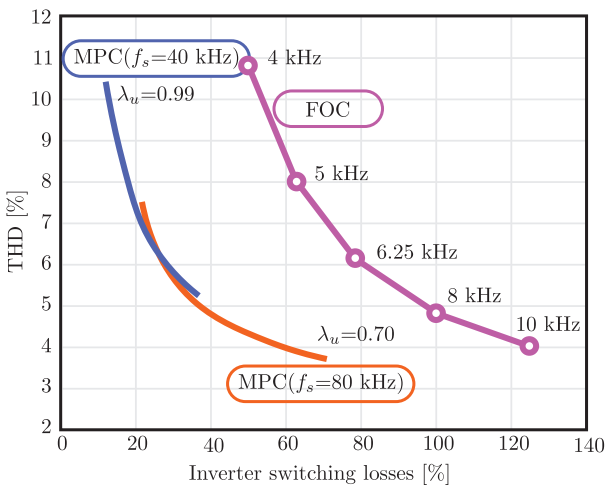

Fig. 18: Inverter switching losses versus THD, reproduced from [35]. Here, f_s refers to the sampling frequency.

Table IV shows a comparison between the inverter losses generated by MPC and FOC in a wide operating range, that it is a summary of the Fig. 8 of [35]. FOC method always generates greater losses in the inverter. Around nominal speed and nominal torque this difference is smaller, however in other operating points this difference is very significant.

Another important requirement for a control scheme in an electromobility application is to reduce the vibrations it generates. In [35] it is shown that the acoustic noise generated by MPC is comparable to linear controller with PWM.

IX. Challenges and Future Work

Until now, MPC has shown that it can be applied in a variety of electrical machines using commercially available microprocessors. And that it works well. The main challenge for MPC is to be adopted by the industry and to achieve this goal it must demonstrate that it offers some advantages in relation to linear control with Pulse Width Modulation (PWM), which is the standard solution. What the industry demands from the control strategy is:

- Ease of application.
- An increase in inverter efficiency.
- Reduction in the distortion of the current supplied to the motor.
- Control of acoustic noise, very important in electric cars.
- Robust behavior against parameter mismatch.
- Be implemented with standard microprocessors.
- Applicability to a wide range of converter systems, including grid-connected converters as well as inverter drive systems.

All these aspects must be addressed in future research. In addition, future work should make a very careful comparison with Field Oriented Control, using linear controllers and PWM and where possible, to demonstrate that it can achieve better results. The comparison must be made independently for each application, converter and motor type. A good result on a drive with a 10 kW induction machine will not necessarily be the best on a 10 MW synchronous machine.

X. Conclusions

The results presented in this paper show that MPC can be adapted to control a wide variety of electrical machines, maintaining the simplicity of the basic control strategy. Particular restrictions and conditions associated with the different types of machines can be easily included by introducing minor changes in the cost functions. Speed, torque, and flux are well controlled in all applications.

A general assessment of the dynamic behavior of the controlled machine shows that model predictive control reaches better results than two well-established high-performance strategies, namely Field Oriented Control and Direct Torque Control.

A more specific assessment in a high-power machine driven by a 3-level neutral point clamped inverter shows that the strategy known as Model Predictive Pulse Pattern Control has superior performance, reducing the inverter losses and the distortion in the motor current when compared with the classical solutions.

Another specific assessment for electric cars shows that multi-step model predictive current control has an outstanding behavior generating less current distortion in the motor, reducing the inverter losses, with a comparable acoustic noise, compared to classical linear control.

As the main conclusion, it can be affirmed that Model Predictive Control emerges as a brilliant and competitive alternative to high-performance strategies for the control of electrical machines.

References

[1] S. Enyedi, “Electric cars — challenges and trends,” in *2018 IEEE International Conference on Automation, Quality and Testing, Robotics (AQTR)*, 2018, pp. 1–8.

[2] F. Altun, S. A. Tekin, S. Gürel, and M. Cernat, “Design and optimization of electric cars. a review of technological advances,” in *2019 8th International Conference on Renewable Energy Research and Applications (ICRERA)*, 2019, pp. 645–650.

[3] A. Emadi, *Advanced Electric Drive Vehicles*, 1st ed. CRC Press, mar 2014.

[4] S. Rachev, D. Stefanov, L. Dimitrov, and D. Koeva, “Evaluation of electric power losses of an induction motor driving a compact electric vehicle at change of parameters and loads,” in *2019 Electric Vehicles International Conference (EV)*, 2019, pp. 1–5.

[5] C. Jiang, M. Qiao, P. Zhu, and Q. Zheng, “Design and verification of high speed permanent magnet synchronous motor for electric car,” in *2018 2nd IEEE Advanced Information Management,Communicates,Electronic and Automation Control Conference (IMCEC)*, 2018, pp. 2371–2375.

[6] F. Zuo, X. Zhang, Y. Zhu, Y. Xu, X. Lv, and C. Qian, "The simulation analysis of control system of pure electric pick-up truck motor," in *2018 IEEE 3rd Advanced Information Technology, Electronic and Automation Control Conference (IAEAC)*, 2018, pp. 1704–1711.

[7] M. Islameka, I. N. Haq, E. Leksono, and B. Yuliarto, "Energy consumption simulation and analysis of rear-driven electric bus with regenerative braking," in *2019 6th International Conference on Electric Vehicular Technology (ICEVT)*, 2019, pp. 105–110.

[8] Z. Ke, J. Zhang, and M. W. Degner, "Dc bus capacitor discharge of permanent-magnet synchronous machine drive systems for hybrid electric vehicles," *IEEE Transactions on Industry Applications*, vol. 53, no. 2, pp. 1399–1405, 2017.

[9] P. Suwanapingkarl, A. Loongthaisong, N. Ritsuk, S. Buasai, C. Paorung, and K. Srivallop, "Motor design for 'epvscooter' an electric scooter integrated with portable photovoltaic charger system," in *2019 International Conference on Power, Energy and Innovations (ICPEI)*, 2019, pp. 1–3.

[10] Y. U. Nugraha, M. N. Yuniarto, H. Herizal, D. A. Asfani, D. C. Riawan, and M. Wahyudi, "Design analysis of axial flux permanent magnet bldc motor 5 kw for electric scooter application," in *2018 International Seminar on Intelligent Technology and Its Applications (ISITIA)*, 2018, pp. 163–168.

[11] L. Wu, W. Ding, and Y. Hu, "Design and analysis of an external-rotor switched reluctance machine for electric bicycle," in *2016 Eleventh International Conference on Ecological Vehicles and Renewable Energies (EVER)*, 2016, pp. 1–6.

[12] G. Sieklucki, "An investigation into the induction motor of tesla model s vehicle," in *2018 International Symposium on Electrical Machines (SME)*, 2018, pp. 1–6.

[13] E. Sokolov, "Comparative study of electric car traction motors," in *2017 15th International Conference on Electrical Machines, Drives and Power Systems (ELMA)*, 2017, pp. 348–353.

[14] P. Rafajdus, A. Peniak, M. Diko, J. Makarovic, P. Dubravka, and V. Hrabovcova, "Using of suitable reluctance motors for electric vehicles and comparison of their performances," in *2015 IEEE 15th International Conference on Environment and Electrical Engineering (EEEIC)*, 2015, pp. 2056–2060.

[15] F. Blaschke, "Apparatus for field-oriented control of asynchronous machines," 4 1971, uS Patent US00283404A. [Online]. Available: https://patents.google.com/patent/US3805135A/en

[16] ——, "The principle of field orientation as applied to the new transvector closed-loop system for rotating-field machines," *Siemens Review*, vol. 34, no. 3, pp. 217–220, 1972.

[17] F. Wang, Z. Zhang, X. Mei, J. Rodríguez, and R. Kennel, "Advanced Control Strategies of Induction Machine: Field Oriented Control, Direct Torque Control and Model Predictive Control," *Energies*, vol. 11, no. 1, p. 120, jan 2018.

[18] F. Wang, X. Mei, J. Rodriguez, and R. Kennel, "Model predictive control for electrical drive systems-an overview," *CES Transactions on Electrical Machines and Systems*, vol. 1, no. 3, pp. 219–230, 2017.

[19] S. Kouro, M. A. Perez, J. Rodriguez, A. M. Llor, and H. A. Young, "Model predictive control: Mpc's role in the evolution of power electronics," *IEEE Industrial Electronics Magazine*, vol. 9, no. 4, pp. 8–21, 2015.

[20] T. Geyer, *Model Predictive Control of High Power Converters and Industrial Drives*, 1st ed. Wiley, 2016.

[21] P. Karamanakos, E. Liegmann, T. Geyer, and R. Kennel, "Model predictive control of power electronic systems: Methods, results, and challenges," *IEEE Open Journal of Industry Applications*, vol. 1, pp. 95–114, 2020.

[22] M. Norambuena, J. Rodriguez, Z. Zhang, F. Wang, C. Garcia, and R. Kennel, "A very simple strategy for high-quality performance of ac machines using model predictive control," *IEEE Transactions on Power Electronics*, vol. 34, no. 1, pp. 794–800, 2019.

[23] L. Chen, S. Huang, J. Guo, Z. Hu, X. Fu, and G. Cao, "Model predictive position control for a planar switched reluctance motor using parametric regression model," in *2019 IEEE International Symposium on Predictive Control of Electrical Drives and Power Electronics (PRECEDE)*, 2019, pp. 1–4.

[24] X. Wang, F. Niu, X. Huang, L. Wu, K. Li, and Y. Fang, "Model parameter online correction method of predictive current control for permanent magnet synchronous motor," in *2019 22nd International Conference on Electrical Machines and Systems (ICEMS)*, 2019, pp. 1–4.

[25] Y. Zhang, Z. Yin, W. Li, X. Tong, and Y. Zhong, "Speed sensorless model predictive control based on disturbance observer for induction motor drives," in *2019 IEEE International Symposium on Predictive Control of Electrical Drives and Power Electronics (PRECEDE)*, 2019, pp. 1–4.

[26] R. Xue, D. Xu, J. Ji, and T. Tao, "Robustness improvement of two-vector-based model predictive current control for permanent magnet synchronous motor," in *2019 22nd International Conference on Electrical Machines and Systems (ICEMS)*, 2019, pp. 1–5.

[27] P. G. Carlet, F. Toso, A. Favato, and S. Bolognani, "A speed and current cascade continuous control set model predictive control architecture for synchronous motor drives," in *2019 IEEE Energy Conversion Congress and Exposition (ECCE)*, 2019, pp. 5682–5688.

[28] T. Geyer, N. Oikonomou, G. Papafotiou, and F. Kieferndorf, "Model predictive pulse pattern control," in *2011 IEEE Energy Conversion Congress and Exposition*, 2011, pp. 3306–3313.

[29] T. Geyer, N. Oikonomou, G. Papafotiou, and F. D. Kieferndorf, "Model predictive pulse pattern control," *IEEE Transactions on Industry Applications*, vol. 48, no. 2, pp. 663–676, 2012.

[30] T. Geyer and N. Oikonomou, "Model predictive pulse pattern control with very fast transient responses," in *2014 IEEE Energy Conversion Congress and Exposition (ECCE)*, 2014, pp. 5518–5524.

[31] N. Oikonomou, C. Gutscher, P. Karamanakos, F. D. Kieferndorf, and T. Geyer, "Model predictive pulse pattern control for the five-level active neutral-point-clamped inverter," *IEEE Transactions on Industry Applications*, vol. 49, no. 6, pp. 2583–2592, 2013.

[32] S. Richter, T. Geyer, and M. Morari, "Resource-efficient gradient methods for model predictive pulse pattern control on an fpga," *IEEE Transactions on Control Systems Technology*, vol. 25, no. 3, pp. 828–841, 2017.

[33] T. Geyer, V. Spudic, W. van der Merwe, and E. Guidi, "Model predictive pulse pattern control of medium-voltage neutral-point-clamped inverter drives," in *2018 IEEE Energy Conversion Congress and Exposition (ECCE)*, 2018, pp. 5047–5054.

[34] M. Vasiladiotis, A. Christe, and T. Geyer, "Model predictive pulse pattern control for modular multilevel converters," *IEEE Transactions on Industrial Electronics*, vol. 66, no. 3, pp. 2423–2431, 2019.

[35] A. Andersson and T. Thiringer, "Assessment of an improved finite control set model predictive current controller for automotive propulsion applications," *IEEE Transactions on Industrial Electronics*, vol. 67, no. 1, pp. 91–100, 2020.

[36] M. Rivera, J. Rodriguez, and S. Vazquez, "Predictive control in power converters and electrical drives—part i," *IEEE Transactions on Industrial Electronics*, vol. 63, no. 6, pp. 3834–3836, 2016.

[37] P. Karamanakos, E. Liegmann, T. Geyer, and R. Kennel, "Model predictive control of power electronic systems: Methods, results, and challenges," *IEEE Open Journal of Industry Applications*, vol. 1, pp. 95–114, 2020.

[38] J. Holtz, "A predictive controller for the stator current vector of ac machines fed from a switched voltage source," *Proc. of IEE of Japan IPEC-Tokyo'83*, pp. 1665–1675, 1983.

[39] M. Depenbrock, "Direct self-control (dsc) of inverter-fed induction machine," *IEEE Transactions on Power Electronics*, vol. 3, no. 4, pp. 420–429, 1988.

[40] E. Flach, R. Hoffmann, and P. Mutschler, "Direct mean torque control of an induction motor," in *European Conference on Power Electronics and Applications*, vol. 3. Proceedings published by various publishers, 1997, pp. 3–672.

[41] P. Cortes, M. P. Kazmierkowski, R. M. Kennel, D. E. Quevedo, and J. Rodriguez, "Predictive control in power electronics and drives," *IEEE Transactions on Industrial Electronics*, vol. 55, no. 12, pp. 4312–4324, 2008.

[42] I. Takahashi and T. Noguchi, "A new quick-response and high-efficiency control strategy of an induction motor," *IEEE Transactions on Industry Applications*, vol. IA-22, no. 5, pp. 820–827, 1986.

[43] S. A. Davari, F. Wang, and R. M. Kennel, "Robust deadbeat control of an induction motor by stable mras speed and stator estimation," *IEEE Transactions on Industrial Informatics*, vol. 14, no. 1, pp. 200–209, 2018.

[44] J. Stumper, V. Hagenmeyer, S. Kuehl, and R. Kennel, "Deadbeat control for electrical drives: A robust and performant design based on differential flatness," *IEEE Transactions on Power Electronics*, vol. 30, no. 8, pp. 4585–4596, 2015.

[45] L. Yan, M. Dou, Z. Hua, H. Zhang, and J. Yang, "Optimal duty cycle model predictive current control of high-altitude ventilator induction motor with extended minimum stator current operation," *IEEE Transactions on Power Electronics*, vol. 33, no. 8, pp. 7240–7251, 2018.

[46] C. Xu, Z. Han, and S. Lu, "Deadbeat predictive current control for permanent magnet synchronous machines with closed-form error

compensation," *IEEE Transactions on Power Electronics*, vol. 35, no. 5, pp. 5018–5030, 2020.

[47] Y. Zhang, J. Jin, and L. Huang, "Model-free predictive current control of pmsm drives based on extended state observer using ultra-local model," *IEEE Transactions on Industrial Electronics*, 2020.

[48] Z. Song, F. Zhou, and Z. Zhang, "Parallel-observer-based predictive current control of permanent magnet synchronous machines with reduced switching frequency," *IEEE Transactions on Industrial Informatics*, vol. 15, no. 12, pp. 6457–6467, 2019.

[49] K. Lee and F. Blaabjerg, "Sensorless dtc-svm for induction motor driven by a matrix converter using a parameter estimation strategy," *IEEE Transactions on Industrial Electronics*, vol. 55, no. 2, pp. 512–521, 2008.

[50] S. A. Davari, D. A. Khaburi, F. Wang, and R. M. Kennel, "Using full order and reduced order observers for robust sensorless predictive torque control of induction motors," *IEEE Transactions on Power Electronics*, vol. 27, no. 7, pp. 3424–3433, 2012.

[51] R. Errouissi, M. Ouhrouche, W.-H. Chen, and A. M. Trzynadlowski, "Robust nonlinear predictive controller for permanent-magnet synchronous motors with an optimized cost function," *IEEE Transactions on Industrial Electronics*, vol. 59, no. 7, pp. 2849–2858, 2012.

[52] T. Türker, U. Buyukkeles, and A. F. Bakan, "A robust predictive current controller for pmsm drives," *IEEE Transactions on Industrial Electronics*, vol. 63, no. 6, pp. 3906–3914, 2016.

[53] R. Kennel, A. Linder, and M. Linke, "Generalized predictive control (gpc)-ready for use in drive applications?" in *2001 IEEE 32nd Annual Power Electronics Specialists Conference (IEEE Cat. No.01CH37230)*, vol. 4, 2001, pp. 1839–1844 vol. 4.

[54] F. Wang, L. He, and J. Rodriguez, "Fpga-based continuous control set model predictive current control for pmsm system using multistep error tracking technique," *IEEE Transactions on Power Electronics*, vol. 35, no. 12, pp. 13 455–13 464, 2020.

[55] A. A. Ahmed, B. K. Koh, and Y. I. Lee, "A comparison of finite control set and continuous control set model predictive control schemes for speed control of induction motors," *IEEE Transactions on Industrial Informatics*, vol. 14, no. 4, pp. 1334–1346, 2018.

[56] X. Luo, A. Shen, Q. Tang, J. Liu, and J. Xu, "Two-step continuous-control set model predictive current control strategy for spmsm sensorless drives," *IEEE Transactions on Energy Conversion*, pp. 1–1, 2020.

[57] D. Kouzoupis, A. Zanelli, H. Peyrl, and H. J. Ferreau, "Towards proper assessment of qp algorithms for embedded model predictive control," in *2015 European Control Conference (ECC)*, 2015, pp. 2609–2616.

[58] G. Cimini, D. Bernardini, S. Levijoki, and A. Bemporad, "Embedded model predictive control with certified real-time optimization for synchronous motors," *IEEE Transactions on Control Systems Technology*, vol. 29, no. 2, pp. 893–900, 2021.

[59] J. Rodriguez, J. Pontt, C. A. Silva, P. Correa, P. Lezana, P. Cortes, and U. Ammann, "Predictive current control of a voltage source inverter," *IEEE Transactions on Industrial Electronics*, vol. 54, no. 1, pp. 495–503, 2007.

[60] S. Kouro, P. Cortes, R. Vargas, U. Ammann, and J. Rodriguez, "Model predictive control—a simple and powerful method to control power converters," *IEEE Transactions on Industrial Electronics*, vol. 56, no. 6, pp. 1826–1838, 2009.

[61] A. Mora, Orellana, J. Juliet, and R. Cárdenas, "Model predictive torque control for torque ripple compensation in variable-speed pmsms," *IEEE Transactions on Industrial Electronics*, vol. 63, no. 7, pp. 4584–4592, 2016.

[62] H. Miranda, P. Cortes, J. I. Yuz, and J. Rodriguez, "Predictive torque control of induction machines based on state-space models," *IEEE Transactions on Industrial Electronics*, vol. 56, no. 6, pp. 1916–1924, 2009.

[63] A. A. Ahmed, "Fast-speed drives for permanent magnet synchronous motor based on model predictive control," in *2015 IEEE Vehicle Power and Propulsion Conference (VPPC)*, 2015, pp. 1–6.

[64] P. Karamanakos, P. Stolze, R. M. Kennel, S. Manias, and H. du Toit Mouton, "Variable switching point predictive torque control of induction machines," *IEEE Journal of Emerging and Selected Topics in Power Electronics*, vol. 2, no. 2, pp. 285–295, 2014.

[65] A. A. Ahmed, B. K. Koh, H. S. Park, K. Lee, and Y. I. Lee, "Finite-control set model predictive control method for torque control of induction motors using a state tracking cost index," *IEEE Transactions on Industrial Electronics*, vol. 64, no. 3, pp. 1916–1928, 2017.

[66] S. A. Davari, M. Norambuena, V. Nekoukar, C. Garcia, and J. Rodriguez, "Even-handed sequential predictive torque and flux control," *IEEE Transactions on Industrial Electronics*, vol. 67, no. 9, pp. 7334–7342, 2020.

[67] Y. Zhang and H. Yang, "Model-predictive flux control of induction motor drives with switching instant optimization," *IEEE Transactions on Energy Conversion*, vol. 30, no. 3, pp. 1113–1122, 2015.

[68] M. Siami, D. Arab Khaburi, and J. Rodriguez, "Simplified finite control set-model predictive control for matrix converter-fed pmsm drives," *IEEE Transactions on Power Electronics*, vol. 33, no. 3, pp. 2438–2446, 2018.

[69] V. P. Muddineni, S. R. Sandepudi, and A. K. Bonala, "Finite control set predictive torque control for induction motor drive with simplified weighting factor selection using topsis method," *IET Electric Power Applications*, vol. 11, no. 5, pp. 749–760, 2017.

[70] M. Norambuena, J. Rodriguez, Z. Zhang, F. Wang, C. Garcia, and R. Kennel, "A very simple strategy for high-quality performance of ac machines using model predictive control," *IEEE Transactions on Power Electronics*, vol. 34, no. 1, pp. 794–800, 2019.

[71] E. Fuentes, C. A. Silva, and R. M. Kennel, "Mpc implementation of a quasi-time-optimal speed control for a pmsm drive, with inner modulated-fs-mpc torque control," *IEEE Transactions on Industrial Electronics*, vol. 63, no. 6, pp. 3897–3905, 2016.

[72] C. F. Garcia, C. A. Silva, J. R. Rodriguez, P. Zanchetta, and S. A. Odhano, "Modulated model-predictive control with optimized overmodulation," *IEEE Journal of Emerging and Selected Topics in Power Electronics*, vol. 7, no. 1, pp. 404–413, 2019.

[73] A. Mora, F. Donoso, M. Urrutia, A. Angulo, and R. Cárdenas, "Predictive control strategy for an induction machine fed by a 3l-npc converter with fixed switching frequency and improved tracking error," in *2018 IEEE 27th International Symposium on Industrial Electronics (ISIE)*, 2018, pp. 155–160.

[74] I. Kim, R. Chan, and S. Kwak, "Model predictive control method for CHB multi-level inverter with reduced calculation complexity and fast dynamics," *IET Electric Power Applications*, vol. 11, no. 5, pp. 784–792, 2017.

[75] B. Bilgin and A. Emadi, "Electric motor industry and switched reluctance machines," in *Switched Reluctance Motor Drives: Fundamentals to Applications*. CRC Press, 2018, ch. 1, pp. 1–34.

[76] H. Chen, S. Xu, and S. Cui, "Reliability Evaluation for Power Converter of SRM on Fault-tolerate Capability and Thermal Stress," *IEEE Transactions on Industrial Electronics*, pp. 1–1, 2020.

[77] J.-W. Ahn and G. F. Lukman, "Switched reluctance motor: Research trends and overview," *CES Transactions on Electrical Machines and Systems*, vol. 2, no. 4, pp. 339–347, Dec. 2018.

[78] B. Burkhart, A. Klein-Hessling, I. Ralev, C. P. Weiss, and R. W. D. Doncker, "Technology, research and applications of switched reluctance drives," *CPSS Transactions on Power Electronics and Applications*, vol. 2, no. 1, pp. 12–27, 2017.

[79] B. Bilgin, B. Howey, A. D. Callegaro, J. Liang, M. Kordic, J. Taylor, and A. Emadi, "Making the case for switched reluctance motors for propulsion applications," *IEEE Transactions on Vehicular Technology*, 2020.

[80] S. Ullah, S. P. McDonald, R. Martin, M. Benarous, and G. J. Atkinson, "A Permanent Magnet Assist, Segmented Rotor, Switched Reluctance Drive for Fault Tolerant Aerospace Applications," *IEEE Transactions on Industry Applications*, vol. 55, no. 1, pp. 298–305, Jan. 2019.

[81] B. Bilgin and A. Emadi, "Electric Motors in Electrified Transportation: A step toward achieving a sustainable and highly efficient transportation system," *IEEE Power Electronics Magazine*, vol. 1, no. 2, pp. 10–17, Jun. 2014.

[82] J. W. Jiang, "Design considerations for switched reluctance machines," in *Switched Reluctance Motor Drives: Fundamentals to Applications*. CRC Press, 2018, ch. 7, pp. 253–315.

[83] E. Bostanci, M. Moallem, A. Parsapour, and B. Fahimi, "Opportunities and Challenges of Switched Reluctance Motor Drives for Electric Propulsion: A Comparative Study," *IEEE Transactions on Transportation Electrification*, vol. 3, no. 1, pp. 58–75, Mar. 2017.

[84] S. Li, S. Zhang, T. G. Habetler, and R. G. Harley, "Modeling, Design Optimization, and Applications of Switched Reluctance Machines—A Review," *IEEE Transactions on Industry Applications*, vol. 55, no. 3, pp. 2660–2681, May 2019.

[85] J. Ye, B. Bilgin, and A. Emadi, "An Offline Torque Sharing Function for Torque Ripple Reduction in Switched Reluctance Motor Drives," *IEEE Transactions on Energy Conversion*, vol. 30, no. 2, pp. 726–735, 2015.

[86] H. Li, B. Bilgin, and A. Emadi, "An Improved Torque Sharing Function for Torque Ripple Reduction in Switched Reluctance Machines," *IEEE Transactions on Power Electronics*, pp. 1–1, 2018.

[87] A. D. Callegaro, B. Bilgin, and A. Emadi, "Radial Force Shaping for Acoustic Noise Reduction in Switched Reluctance Machines," *IEEE Transactions on Power Electronics*, pp. 1–1, 2019.

[88] D. F. Valencia, S. R. Filho, A. D. Callegaro, M. Preindl, and A. Emadi, "Virtual-Flux Finite Control Set Model Predictive Control of Switched Reluctance Motor Drives," in *IECON 2019 - 45th Annual Conference of the IEEE Industrial Electronics Society*, vol. 1, Oct. 2019, pp. 1465–1470.

[89] X. Li and P. Shamsi, "Model Predictive Current Control of Switched Reluctance Motors With Inductance Auto-Calibration," *IEEE Transactions on Industrial Electronics*, vol. 63, no. 6, pp. 3934–3941, 2016.

[90] C. Li, G. Wang, Y. Li, and A. Xu, "An improved finite-state predictive torque control for switched reluctance motor drive," *IET Electric Power Applications*, vol. 12, no. 1, pp. 144–151, 2018.

[91] R. Abdel-Fadil and L. Számel, "Enhancement Of the Switched Reluctance Motor Performance for Electric Vehicles Applications Using Predictive Current Control," in *2018 International IEEE Conference and Workshop in Óbuda on Electrical and Power Engineering (CANDO-EPE)*, Nov. 2018, pp. 000 195–000 200.

[92] S. Song, R. Hei, R. Ma, and W. Liu, "Model Predictive Control of Switched Reluctance Starter/Generator with Torque Sharing and Compensation," *IEEE Transactions on Transportation Electrification (early access)*, pp. 1–1, 2020.

[93] R. Tarvirdilu-Asl, S. Nalakath, B. Bilgin, and A. Emadi, "A Finite Control Set Model Predictive Torque Control for Switched Reluctance Motor Drives with Adaptive Turn-off Angle," in *IECON 2019 - 45th Annual Conference of the IEEE Industrial Electronics Society*, vol. 1, Oct. 2019, pp. 840–845.

[94] X. Li and P. Shamsi, "Inductance Surface Learning for Model Predictive Current Control of Switched Reluctance Motors," *IEEE Transactions on Transportation Electrification*, vol. 1, no. 3, pp. 287–297, 2015.

[95] M. G. Bijan, M. Al-Badri, P. Pillay, and P. Angers, "Induction machine parameter range constraints in genetic algorithm based efficiency estimation techniques," *IEEE Transactions on Industry Applications*, vol. 54, no. 5, pp. 4186–4197, 2018.

[96] K. Wang, Y. Li, Q. Ge, and L. Shi, "An improved indirect field-oriented control scheme for linear induction motor traction drives," *IEEE Transactions on Industrial Electronics*, vol. 65, no. 12, pp. 9928–9937, 2018.

[97] W. Xu, R. Islam, and M. Pucci, *Advanced Linear Machines and Drive Systems*, 1st ed. Springer-Verlag Berlin Heidelberg, Aug. 2019.

[98] W. Xu, J. Zou, Y. Liu, and J. Zhu, "Weighting factorless model predictive thrust control for linear induction machine," *IEEE Transactions on Power Electronics*, vol. 34, no. 10, pp. 9916–9928, 2019.

[99] J. Zou, W. Xu, X. Yu, Y. Liu, and C. Ye, "Multistep model predictive control with current and voltage constraints for linear induction machine based urban transportation," *IEEE Transactions on Vehicular Technology*, vol. 66, no. 12, pp. 10 817–10 829, 2017.

[100] J. Zou, W. Xu, J. Zhu, and Y. Liu, "Low-complexity finite control set model predictive control with current limit for linear induction machines," *IEEE Transactions on Industrial Electronics*, vol. 65, no. 12, pp. 9243–9254, 2018.

[101] ——, "Simplified model predictive thrust control based arbitrary two voltage vectors for linear induction machines in metro transportation," *IEEE Transactions on Vehicular Technology*, vol. 69, no. 7, pp. 7092–7103, 2020.

[102] J. Zou, W. Xu, and C. Ye, "Improved deadbeat control strategy for linear induction machine," *IEEE Transactions on Magnetics*, vol. 53, no. 6, pp. 1–4, 2017.

[103] J. Zou and W. Xu, "Optimal current reference with maximum thrust criterion for linear induction machine based deadbeat control," in *IECON 2017 - 43rd Annual Conference of the IEEE Industrial Electronics Society*, 2017, pp. 3682–3687.

[104] W. Xu, M. F. Elmorshedy, Y. Liu, M. R. Islam, and S. M. Allam, "Finite-set model predictive control based thrust maximization of linear induction motors used in linear metros," *IEEE Transactions on Vehicular Technology*, vol. 68, no. 6, pp. 5443–5458, 2019.

[105] W. Xu, M. F. Elmorshedy, Y. Liu, J. Rodriguez, and C. Garcia, "Maximum thrust per ampere of linear induction machine based on finite-set model predictive direct thrust control," *IEEE Transactions on Power Electronics*, vol. 35, no. 7, pp. 7366–7378, 2020.

[106] M. Elmorshedy, W. Xu, S. M. Allam, J. Rodriguez, and C. Garcia, "Mtpa-based finite-set model predictive control without weighting factors for linear induction machine," *IEEE Transactions on Industrial Electronics*, pp. 1–1, 2020.

[107] F. Barrero and M. J. Duran, "Recent advances in the design, modeling, and control of multiphase machines—Part I," *IEEE Transactions on Industrial Electronics*, vol. 63, no. 1, pp. 449–458, 2016.

[108] M. J. Duran and F. Barrero, "Recent advances in the design, modeling, and control of multiphase machines—Part II," *IEEE Transactions on Industrial Electronics*, vol. 63, no. 1, pp. 459–468, 2016.

[109] E. Levi, "Advances in converter control and innovative exploitation of additional degrees of freedom for multiphase machines," *IEEE Transactions on Industrial Electronics*, vol. 63, no. 1, pp. 433–448, 2016.

[110] J. Rodas, F. Barrero, M. R. Arahal, C. Martín, and R. Gregor, "Online estimation of rotor variables in predictive current controllers: A case study using five-phase induction machines," *IEEE Transactions on Industrial Electronics*, vol. 63, no. 9, pp. 5348–5356, 2016.

[111] J. Rodas, C. Martín, M. R. Arahal, F. Barrero, and R. Gregor, "Influence of covariance-based ALS methods in the performance of predictive controllers with rotor current estimation," *IEEE Transactions on Industrial Electronics*, vol. 64, no. 4, pp. 2602–2607, 2017.

[112] M. Ayala, J. Doval-Gandoy, J. Rodas, O. Gonzalez, R. Gregor, and M. Rivera, "A novel modulated model predictive control applied to six-phase induction motor drives," *IEEE Transactions on Industrial Electronics*, pp. 1–1, 2020.

[113] M. R. Arahal, F. Barrero, M. J. Duran, M. G. Ortega, and C. Martín, "Trade-offs analysis in predictive current control of multi-phase induction machines," *Control Engineering Practice*, vol. 81, pp. 105–113, 2018.

[114] M. J. Duran, J. A. Riveros, F. Barrero, H. Guzman, and J. Prieto, "Reduction of common-mode voltage in five-phase induction motor drives using predictive control techniques," *IEEE Transactions on Industry Applications*, vol. 48, no. 6, pp. 2059–2067, 2012.

[115] J. A. Riveros, F. Barrero, E. Levi, M. J. Durán, S. Toral, and M. Jones, "Variable-speed five-phase induction motor drive based on predictive torque control," *IEEE Transactions on Industrial Electronics*, vol. 60, no. 8, pp. 2957–2968, 2013.

[116] J. J. Aciego, I. González Prieto, and M. J. Duran, "Model predictive control of six-phase induction motor drives using two virtual voltage vectors," *IEEE Journal of Emerging and Selected Topics in Power Electronics*, vol. 7, no. 1, pp. 321–330, 2019.

[117] O. Gonzalez, M. Ayala, J. Doval-Gandoy, J. Rodas, R. Gregor, and M. Rivera, "Predictive-fixed switching current control strategy applied to six-phase induction machine," *Energies*, vol. 12, no. 12, p. 2294, 2019.

[118] P. Gonçalves, S. Cruz, and A. Mendes, "Finite control set model predictive control of six-phase asymmetrical machines—an overview," *Energies*, vol. 12, no. 24, p. 4693, 2019.

[119] M. Bermúdez, C. Martín, I. González-Prieto, M. J. Durán, M. R. Arahal, and F. Barrero, "Predictive current control in electrical drives: an illustrated review with case examples using a five-phase induction motor drive with distributed windings," *IET Electric Power Applications*, vol. 14, no. 8, pp. 1291–1310, 2020.

[120] J. Rodriguez, R. M. Kennel, J. R. Espinoza, M. Trincado, C. A. Silva, and C. A. Rojas, "High-performance control strategies for electrical drives: An experimental assessment," *IEEE Transactions on Industrial Electronics*, vol. 59, no. 2, pp. 812–820, 2012.

[121] F. Wang, Z. Chen, P. Stolze, R. Kennel, M. Trincado, and J. Rodriguez, "A comprehensive study of direct torque control (dtc) and predictive torque control (ptc) for high performance electrical drives," *Epe Journal*, vol. 25, no. 1, pp. 12–21, 2015.

[122] F. Wang, S. Li, X. Mei, W. Xie, J. Rodríguez, and R. M. Kennel, "Model-based predictive direct control strategies for electrical drives: An experimental evaluation of ptc and pcc methods," *IEEE Transactions on Industrial Informatics*, vol. 11, no. 3, pp. 671–681, 2015.

[123] G. S. Buja, "Optimum output waveforms in pwm inverters," *IEEE Trans. Ind. Appl.*, vol. IA-16, no. 6, pp. 830–836, 1980.

[124] G. S. Buja and M. P. Kazmierkowski, "Direct torque control of pwm inverter-fed ac motors - a survey," *IEEE Transactions on Industrial Electronics*, vol. 51, no. 4, pp. 744–757, 2004.

[125] T. Geyer, G. Papafotiou, and M. Morari, "Model predictive direct torque control–part i: Concept, algorithm, and analysis," *IEEE Transactions on Industrial Electronics*, vol. 56, no. 6, pp. 1894–1905, 2009.

[126] T. Geyer and D. E. Quevedo, "Multistep finite control set model predictive control for power electronics," *IEEE Transactions on Power Electronics*, vol. 29, no. 12, pp. 6836–6846, 2014.

[127] A. Ayad, P. Karamanakos, and R. Kennel, "Direct model predictive current control strategy of quasi-z-source inverters," *IEEE Transactions on Power Electronics*, vol. 32, no. 7, pp. 5786–5801, 2017.

[128] P. Acuna, C. A. Rojas, R. Baidya, R. P. Aguilera, and J. E. Fletcher, "On the impact of transients on multistep model predictive control for medium-voltage drives," *IEEE Transactions on Power Electronics*, vol. 34, no. 9, pp. 8342–8355, 2019.
[129] T. Geyer and D. E. Quevedo, "Performance of multistep finite control set model predictive control for power electronics," *IEEE Transactions on Power Electronics*, vol. 30, no. 3, pp. 1633–1644, 2015.
[130] T. Dorfling, H. du Toit Mouton, T. Geyer, and P. Karamanakos, "Long-horizon finite-control-set model predictive control with nonrecursive sphere decoding on an fpga," *IEEE Transactions on Power Electronics*, vol. 35, no. 7, pp. 7520–7531, 2020.
[131] P. Karamanakos and T. Geyer, "Guidelines for the design of finite control set model predictive controllers," *IEEE Transactions on Power Electronics*, vol. 35, no. 7, pp. 7434–7450, 2020.

Jorge Rodas (S'08–M'12–SM'19) received his M.Sc. degrees from the Universidad de Vigo, Spain, in 2012 and from the Universidad de Sevilla, Spain, in 2013, and his joint-university Ph.D. degree between the Universidad Nacional de Asunción and the Universidad de Sevilla in 2016. In 2011, he joined the Universidad Nacional de Asuncion, Paraguay, where he currently serves as a professor. His research interests focus on applications of advanced control to real-world problems. Current research activities include applying model-based predictive control and nonlinear control to power electronic converters, renewable energy conversion systems, electric motor drives and robotic systems (especially drones).

Diego Valencia (S'12–M'21) received the Ph.D. degree in electrical engineering from McMaster University, Hamilton, ON, Canada in 2021. He is currently a Postdoctoral Research Fellow at the McMaster Automotive Resource Center (MARC). His current research interests include control of electric motor drives and power electronics for electrified transportation and model predictive control of power converters and drives.

Mahmoud F. Elmorshedy (S'19–M'21) was born in Gharbeya, Egypt in 1989. He received both B.Sc. and M.Sc. degrees in electrical engineering from Tanta University, Egypt, in 2012 and 2016, and the Ph.D. from Huazhong University of Science and Technology, China, in 2020, respectively. He started working as a teaching assistant at the Department of Electrical Power and Machines Engineering, Tanta University in 2013. In June 2016, He was promoted to the degree of assistant lecturer in the same department. Currently, He is working as an Assistant Professor at the Department of Electrical Power and Machines Engineering, Faculty of Engineering, Tanta University. His research interests include linear induction motor, predictive control, power electronics, and renewable energy.

Kunkun Zuo received the M.S. degree in control engineering from University of Chinese Academy of SciencesChina. He is currently working toward the Ph.D. degree in Institute of Electrical Drive Systems and Power Electronics, Technical University of Munich, Germany.

His research interests include model predictive control, disturbance observer, and power optimization control for electrical drive systems.

Wei Xu (M'09-SM'13) received the double B.E. and M.E. degrees from Tianjin University, Tianjin, China, in 2002 and 2005, and the Ph.D. from the Institute of Electrical Engineering, Chinese Academy of Sciences, in 2008, respectively, all in electrical engineering. His research topics mainly cover design and control of linear/rotary machines.

From 2008 to 2012, he made Postdoctoral Fellow with University of Technology Sydney, Vice Chancellor Research Fellow with Royal Melbourne Institute of Technology, Japan Science Promotion Society Invitation Fellow with Meiji University, respectively. Since 2013, he has been full professor with State Key Laboratory of Advanced Electromagnetic Engineering in Huazhong University of Science and Technology, China. He has more than 110 papers accepted or published in IEEE Journals, two edited books published by Springer Press, one monograph published by China Machine Press, and more than 150 Invention Patents granted or in pending, all in the related fields of electrical machines and drives. He is Fellow of the Institute of Engineering and Technology (IET). He is the General Chair for 2021 International Symposium on Linear Drives for Industry Applications (LDIA 2021) and 2023 IEEE International Conference on Predictive Control of Electrical Drives and Power Electronics (PRECEDE 2023) in Wuhan, China, respectively. He has been Associate Editor for several leading IEEE Transactions Journals, such as IEEE Transactions on Industrial Electronics, IEEE Transactions on Vehicular Technology, IEEE Transactions on Energy Conversion, and so on.

Ali Emadi (IEEE S'98-M'00-SM'03-F'13) is the Canada Excellence Research Chair Laureate at McMaster University in Hamilton, Ontario, Canada. He is also the holder of the NSERC/Stellantis Industrial Research Chair in Electrified Powertrains and Tier I Canada Research Chair in Transportation Electrification and Smart Mobility. Before joining McMaster University, Dr. Emadi was the Harris Perlstein Endowed Chair Professor of Engineering and Director of the Electric Power and Power Electronics Center and Grainger Laboratories at Illinois Institute of Technology in Chicago, Illinois, USA. He was the founding Editor-in-Chief of the IEEE Transactions on Transportation Electrification from 2014 to 2020.